http://ansinet.com/itj

ITJ

ISSN 1812-5638

INFORMATION TECHNOLOGY JOURNAL

ANSInet
Asian Network for Scientific Information
308 Lasani Town, Sargodha Road, Faisalabad - Pakistan

Information Technology Journal 12 (10): 1941-1949, 2013
ISSN 1812-5638 / DOI: 10.3923/itj.2013.1941.1949

Study on Unified S Band Receiver Performance with Impulse Radio Ultra-wideband Disturbance

Zhilu Wu, Lei Xu and Zhendong Yin
School of Electronics and Information Technology, Harbin Institute of Technology,
Harbin, Heilongjiang 150001, China

Abstract: Ultra-Wideband (UWB) is widely used in wireless communication systems while Unified S-band (USB) receivers are often used in the tracking, telemetry and command (TT and C) system. In this paper, unlike conventional applications, the UWB signals are employed as interference signals to a USB model. This study focuses on the performance of USB receiver under the interference situation of IR-UWB communication signal and the Signal-to-Interference Ratio (SIR) threshold is analyzed in different Signal-to-Noise Ratio (SNR). Furthermore, an appropriate Soft-Spectrum Adaptation (SSA) method is employed to design the ultra-wideband (UWB) signal and the UWB pulse can cover the entire S-band. Simultaneously, it researches the performance of USB receiver under the UWB pulse interference. Our studies and performance results show a referenced threshold for both the anti-interference of USB receiver and UWB signal interfere receiver.

Key words: UWB interference, waveform design, SSA, united S-band receiver, BER

INTRODUCTION

Currently, Ultra-Wideband (UWB) Communication is a powerful and promising technique in the field of wireless communication. The Ultra Wide-Band (UWB) signal is defined as any signal that occupies more than 500 MHZ of spectrum or has a fractional bandwidth in excess of 20% (FCC, 2002). UWB signal has low average transmit power, wide bandwidth and low Power Spectrum Density (PSD), it can be submerged in the noise (Wu *et al*., 2008). UWB communication systems have the following advantages such as high throughput due to the wide occupied bandwidth, low power consumption decision by limits on transmit power spectral density, accurate position/timing location communications capabilities, excellent multi-path fading robustness afforded by the short impulse and low-cost implementations (Foerster *et al*., 2001). UWB signals spread across a very wide bandwidth and could be made to appear as noise to most interception equipment (Li *et al*., 2011). Recently, the issue of outer space formation flying has obtained more and more attention with the rapid growth of outer space technology (Liu and Li, 2009). Establishing the inter-aircraft wireless communication is one of the key technologies in the formation flying. The advantages of direct sequence designs are low computational complexities and easily implementation in practical systems (Hua and Beaulieu, 2011). Constructing the communication links of formation flying aircrafts has many means, direct-sequence ultra-wideband (DS-UWB) technology is a proper one (Yin *et al*., 2012).

As one of the seven systems in manned space system, United S-Band (USB) communication system plays a crucial role. United S-Band receiver is the most important components of the system which is used to amplify the received signal and convert it to low frequency. The S-band services for commercial and military radars for a long time because of its high performance and reliability (Peng *et al*., 2011).

The most remarkable advantage of the DS-UWB communication system is high communication capacity and good multiple access multiplexing capability. Taking into account the development of space satellite technology and the formation aircraft technology, the main star-ground monitoring and control system is still the Unified S-band Telemetry Tracking and Control System. Compared with the ultra-wideband signals the USB signals are narrowband signals which may be the strong narrowband interferences (NBI) to affect the UWB system (Wang *et al*., 2010). Therefore, it must be considered the coexistence of the two systems when researching the DS-UWB communication system.

This study first designs the SSA pulse waveform based on Gaussian derivatives and Prolate Spheroidal Wave Functions (PSWF), simultaneously, the UWB pulse waveforms designed cover the entire S-band and uses the

Corresponding Author: Zhendong Yin, School of Electronics and Information Technology, Harbin Institute of Technology, Harbin, Heilongjiang 150001, China Tel: (+86)13019705608

UWB pulse signals as interference signals. Then, it designs the transmitter and receiver model of the Unified S-band system and researches the performance of USB receiver.

PULSE DESIGN FOR UWB WAVEFORM

UWB pulse design based on Gaussian derivatives: Typical UWB pulse waveform is generated by the Gaussian Monocycle pulse. A lot of literatures related to UWB communications analyze its performance. Initially, most of the UWB pulses are similar to the Gaussian pulse. Therefore, the Gaussian pulse become a traditional UWB signal (Parr *et al*., 2003). Gaussian function can be defined as:

$$f(t) = \pm\frac{\sqrt{2}}{\alpha^2}\exp\left(-\frac{2\pi t^2}{\alpha^2}\right) \quad (1)$$

where, $\alpha^2 = 4\pi\sigma^2$ is pulse shaping factor, σ^2 is variance. Reducing the value of α will compress the pulse width and increasing the value causes the pulse width increasing. Therefore, α can affect the pulse width and amplitude. When pulse shaping factor α changed, Gaussian pulse was a binary function. Supposing that the minimum of α equaled to 0.414×10^{-9}, the changing step length of α equaled to 0.1×10^{-9} and α changed six times continuously. Generated waveforms of Gaussian pulse in time domain and frequency domain were illustrated in Fig. 1. It shows the pulse width decreasing with α increasing.

Its energy expression is:

$$E_p = \int_{-\infty}^{+\infty} f^2(t)dt = A_p^2\int_{-\infty}^{+\infty}\exp\left(-\frac{4\pi t^2}{\alpha^2}\right)dt = \frac{A_p^2\alpha}{2} \quad (2)$$

It can be seen when:

$$A_p = \pm\sqrt{\frac{2}{\alpha}}$$

energy $E_p = 1$.

Spectral characteristics of the Gaussian pulse and k-order Gaussian pulse as following:

$$f(t) \leftrightarrow \pm A_p\frac{\alpha}{\sqrt{2}}\exp\left(-\frac{\alpha^2\omega^2}{8\pi}\right) \quad (3)$$

$$f^{(k)}(t) \leftrightarrow \pm A_p\frac{\alpha}{\sqrt{2}}\exp\left(-\frac{\alpha^2\omega^2}{8\pi}\right)(j\omega)^k \quad (4)$$

The expression of gaussian derivative changed with the derivative order. To explain the influence, the time domain and frequency domain waveform of first-ninth derivative Gaussian pulse was illustrated in Fig. 2 where α equaled to 0.714×10^{-9}. It is easy to know the PSD removes to higher frequency with the augment of Gaussian derivative function's order. What's more, the changing of pulse shaping factor can adjust gaussian pulse shape and the different order derivative of gaussian pulse can gain lots of different waveforms. So the linear combination of Gaussian waveforms can generate the UWB pulse which meet the conditions.

SSA pulse design based on prolate spheroidal wave functions: The formation flying aircrafts communication system in the outer space, since the FCC required template is not suitable in this situation. The Soft Spectrum Adaptation (SSA) algorithm has a good capacity of match for any power spectrum template

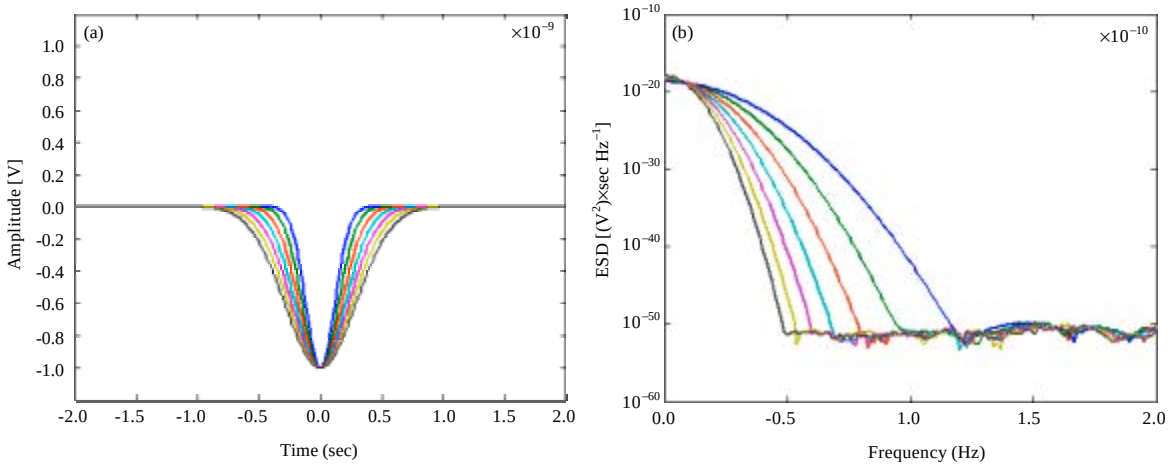

Fig. 1(a-b): Gaussian pulse changed with α (a) Time domain and (b) Frequency domain

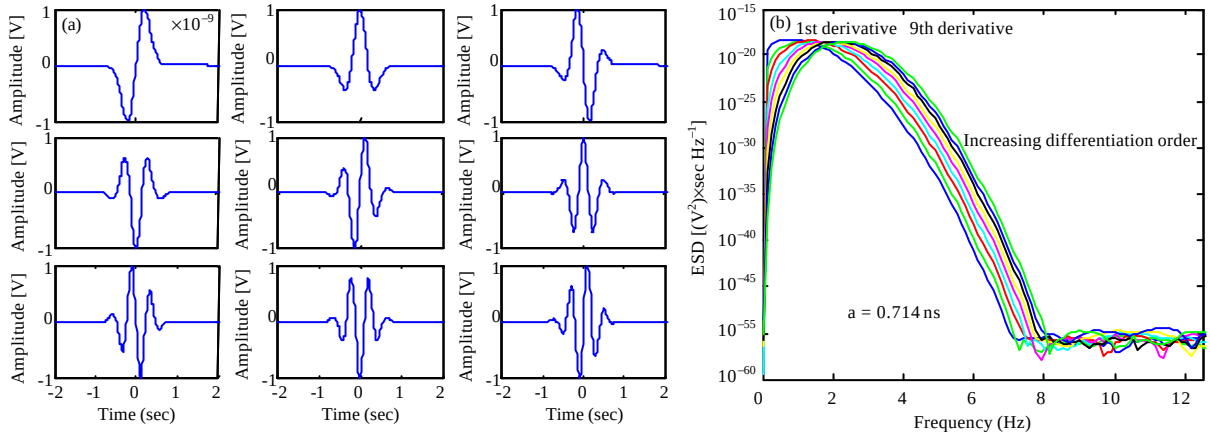

Fig. 2(a-b): The 1-9 order Gaussian pulse shape in (a) Time domain and (b) Frequency domain

adaptively. The soft spectrum adaptation algorithm is an optimized waveform design to meet the requirements of co-existence and interference avoidance. It can adaptive design waveform, the structure of the waveform can be adjusted on demand at any time. Considering the literature (Parr *et al*., 2003; Honggang and Kohno, 2003; Slepian, 1983; Lei *et al*., 2010; Di *et al*., 2010),we use core wavelet sequence based on PSWF to constitute the UWB pulse waveforms.

This algorithm divides S-band into n sub-bands and selects any one sub-band. The time domain and frequency domain of the kth sub-band simplified as following:

$$h_k(t) = 2f_{k,H}\,\mathrm{sin\,c}(2f_{k,H}t) - 2f_{k,L}\,\mathrm{sin\,c}(2f_{k,L}t) \tag{5}$$

$$H_k(f) = \begin{cases} 1, & f_{k,L} \le f \le f_{k,H} \\ 0, & \text{elsewise} \end{cases} \tag{6}$$

where, $f_{k,H}$ and $f_{k,L}$ denote the high and low frequency, respectively. And the output of the impulse filter can be defined as:

$$\lambda_k \varphi_k(t) = \int_{-\infty}^{\infty} \varphi_k(\tau) h_k(t-\tau) d\tau \tag{7}$$

where, λ_k is an arbitrary constant:

$$h_k(t) = \frac{\sin W_k(t)}{t}$$

where, W_k is the bandwidth of the kth sub-band. And $\varphi_k(\tau)$ is prolate spheroidal wave functions which are designed to be time-limited and energy-concentrated over the pulse width $[-T_p/2, T_p/2]$, Eq. 7 can be expressed as:

$$\lambda_k \varphi_k(t) = \int_{-T_p/2}^{T_p/2} \varphi_k(\tau) \frac{\sin W_k(t-\tau)}{t-\tau} d\tau \tag{8}$$

It is difficult to find the solution of Eq. 8, other literatures proposed discrete algorithm. Equation 7 can be expressed as following:

$$\lambda_k \varphi_k[n] = \sum_{m=-N/2}^{N/2} \varphi_k[m] h_k[n-m], n = -N/2, \cdots, N/2 \tag{9}$$

Upon expression in vector form, quality Eq. 9 becomes a matrix multiplication form of $\lambda_k\varphi_k = H\varphi_k$ with H and the sample vector φ_k as follows:

$$\lambda_k \begin{bmatrix} \varphi[-\frac{N}{2}] \\ \varphi[-\frac{N}{2}+1] \\ \cdots \\ \varphi[0] \\ \cdots \\ \varphi[\frac{N}{2}] \end{bmatrix} = \begin{bmatrix} h[0] & h[-1] & \cdots & h[-N] \\ h[1] & h[0] & \cdots & h[-N+1] \\ \cdots & \cdots & \cdots & \cdots \\ h[\frac{N}{2}] & h[\frac{N}{2}-1] & \cdots & h[-\frac{N}{2}] \\ \cdots & \cdots & \cdots & \cdots \\ h[N] & h[N-1] & \cdots & h[0] \end{bmatrix} \begin{bmatrix} \varphi[-\frac{N}{2}] \\ \varphi[-\frac{N}{2}+1] \\ \cdots \\ \varphi[0] \\ \cdots \\ \varphi[\frac{N}{2}] \end{bmatrix} \tag{10}$$

where, φ_k is an eigenvector of H. Define φ_k as $[\varphi_1, \varphi_2, \ldots, \varphi_k]$ and λ_k as $[\lambda_1, \lambda_2, \ldots, \lambda_k]$, where the eigenvalues are arranged in descending order.

SIMULATION RESULTS

This study divides 2~4 GHz into 4 sub-bands and simulates every sub-band to get PSWF-based orthogonal pulse waveforms. It just needs to get the maximum eigenvalue vector for the calculation of matrix. To improve computation efficiency, the study replaces the traditional matlab method by this Power Method which reduces largely calculating time without losing accuracy.

The UWB pulses waveforms are plotted in Fig. 3. As shown in Fig. 3, with the increasing in high and low frequency, respectively, waveforms in time domain are more complicated and the center frequency of waveforms in frequency domain increases. Figure 4 shows the PSD of the combination wave, given by:

$$\varphi_{mul}(t) = \sum_{k=1}^{4} \varphi_k(t) \quad (11)$$

where, $\varphi_k(t)$ is the optimized wavelet in Fig. 3. Waveforms cover the entire S-band 1.55-3.4 GHz and the center frequency is about 2.1 GHz.

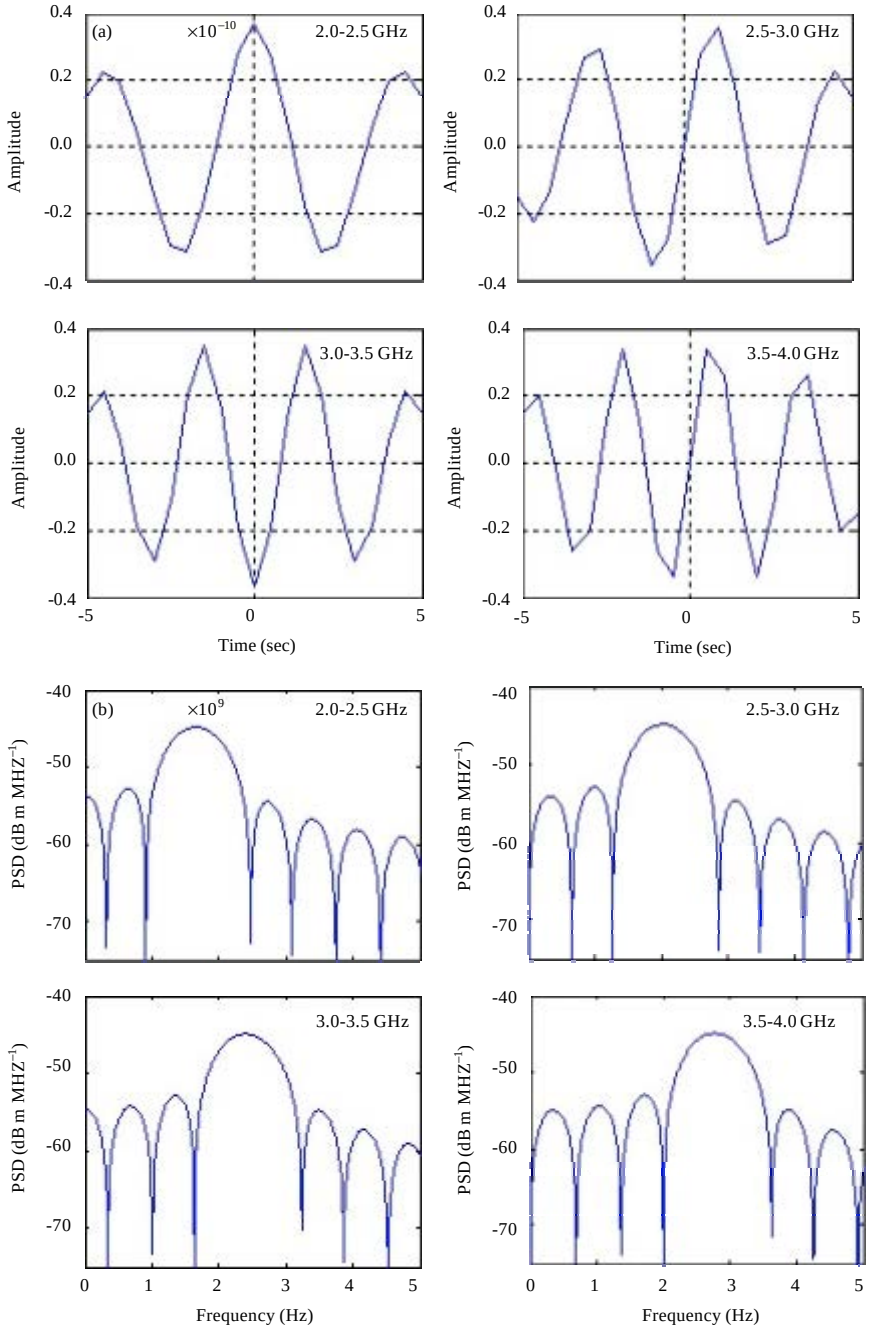

Fig. 3(a-b): Optimized pulse waveforms generation based on PSWF in (a) Time domain and (b) Frequency domain

USB COMMUNICATION SIMULATION SYSTEM DESIGN AND ANALYSIS

The establishment of the simulation system: In communication simulation system, the transmitter model of the USB communication simulation system (Fig. 5) is composed of the simulation modules of the PCM coding, spread spectrum, BPSK modulation, signal synthesis, the PM modulation and filtering. Transmitted signal S(t) can be expressed as:

$$S(n) = \sqrt{2P}\cos(2\pi f_{sc}t + m_p s(n)c(n)\cos(2\pi f_c t)) \quad (12)$$

where, s(n) is baseband signal, c(n) is spread-spectrum signal, f_c and f_{sc} is the subcarrier frequency and the main carrier frequency, respectively, m_p is phase modulation index, P is the transmitted signal power, t is the duration after sampling $t\in\{0, 1,...,q\}/f_{s1}$, where f_{s1} is sampling frequency. The received signal $S_n(n)$ can be expressed as:

$$S_n(n) = S(n)+N(n)+I(n) \quad (13)$$

where, N(n) is white Gaussian noise, I(n) is other signal interference. Figure 5 shows the receiver model of the USB communication simulation system. First, the received signal $S_n(n)$ goes through the front-end RF filter of the receiver. Then, it passes PM demodulation, down-sampling, phase demodulation, BPSK coherent demodulation, low pass filtering and judgment module successively. At last, the Bit Error Rate (BER) of United S-Band receiver is outputted.

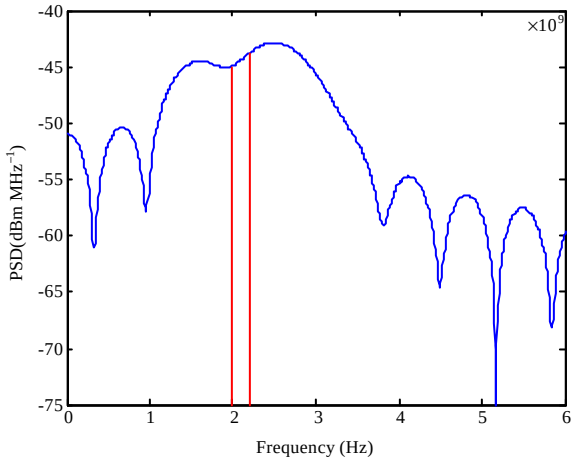

Fig. 4: Power spectrum density of designed UWB-pulse

SIMULATION AND ANALYSIS

Based on the above simulation model, the simulation parameters as follows: The baseband signal sampling frequency $f_{s1} = 4\times10^8$ Hz, Baseband code rate $f_d = 4\times10^6$Hz, Subcarrier frequency $f_c = 4\times10^7$Hz, The main carrier frequency $f_{sc} = 2.1\times10^9$ Hz, Baseband symbol length S = 10000, Down-sampling frequency $f_{s1} = 4\times10^8$ Hz, Pulse amplitude modulation using bipolar NRZ modulation, Number of cycles is 100.

The transmitted signal spectrum of Baseband signal modulated by PM and BPSK is illustrated in Fig. 6.

The Fig. 7 shows a deteriorate curve of system performance when the Unified S-band receiver is disturbed by Gaussian white noise. If SNR is above 5.2 dB, the USB receiver has a good performance, because of the USB receiver with a degree of anti-jamming capability. With the noise power increasing gradually, the performance of the USB receiver will be worse. The receiver is not available when the signal-to-noise ratio is less than 5 dB.

The emission and receiving process of the signals is similar to the model above, the difference is that the receiver also receives UWB interference signals when the receiver receives the transmitted signals. Here the UWB interference signals are the ones designed in the Chapter II. Ultra-wideband signal sampling frequency f_s is much higher than the baseband code rate f_d and the sampling frequency of the baseband code f_{s1}. Therefore, ultra wideband signal needs down-sampling so that the frequency declines to the sampling frequency of the USB signal. Ultra-wideband signal covers the entire S-band and interference signals only need to cover transmit signal bandwidth, so the ultra-wideband signal energy can be concentrated by band-pass filter.

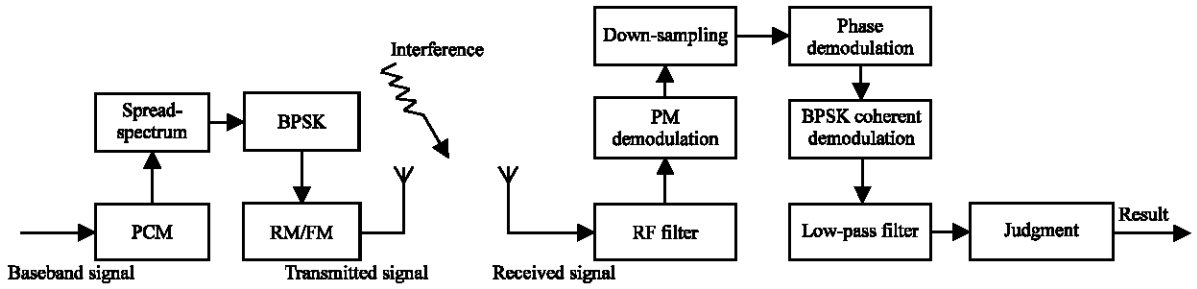

Fig. 5: USB communication simulation system

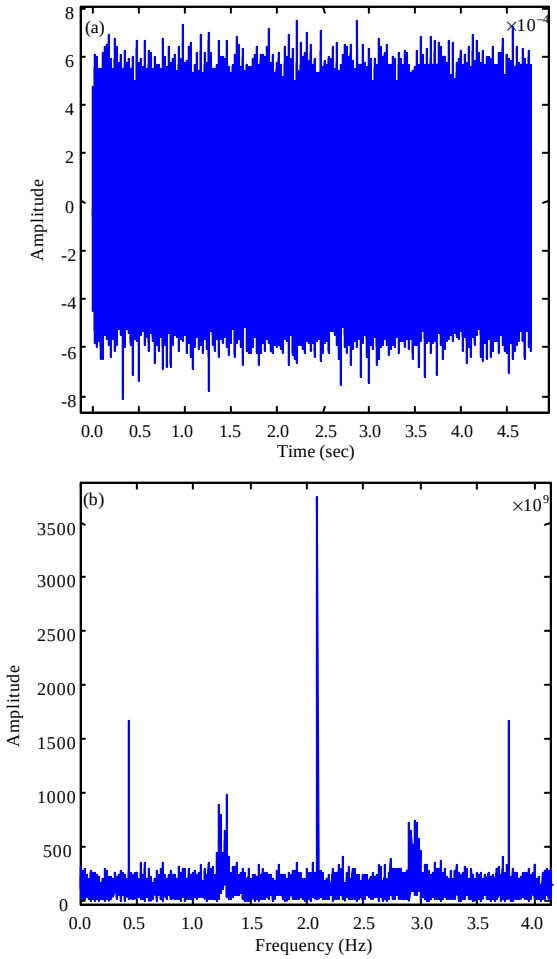

Fig. 6(a-b): Transmitted signals in (a) Time domain and (b) Frequency domain

The other simulation parameters are unchanged. According to the above simulation results, the USB receiver can work properly when the SNR is above 5.2 dB, so the following simulation selects 6, 7 and 8 dB. Figure 8 shows the time domain and frequency domain waveforms of the BPSK and PM modulated emission signal which added UWB interference and AWGN interference.

Figure 9 gives the contrast curves of system performance of the Unified S-band receiver interfered by the ultra-wideband signal in different SNR. In Fig. 9, Signal to Interference Ratio (SIR) is the useful signal power divided by the interference signal power before the receiver band-pass filter. The bandwidth of interference signal is 2.4 Ghz. The bandwidth of useful signal is 40 MHZ. So, the SIR after the band-pass filter should subjoin 10 log $(2.4\times10^3/40)$ = 17.8 dB. Following conclusions can be obtained from the figure:

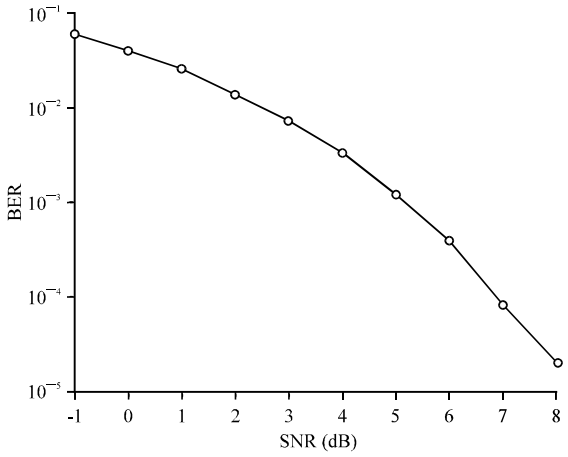

Fig. 7: USB receiver performance curve

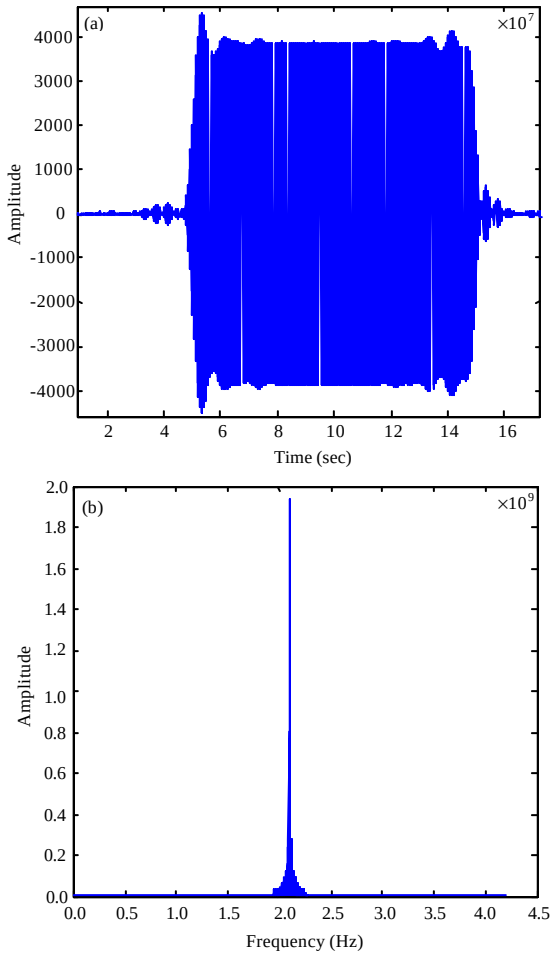

Fig. 8(a-b): Waveforms of the emission signal added interferences (a) Time domain and (b) Frequency domain

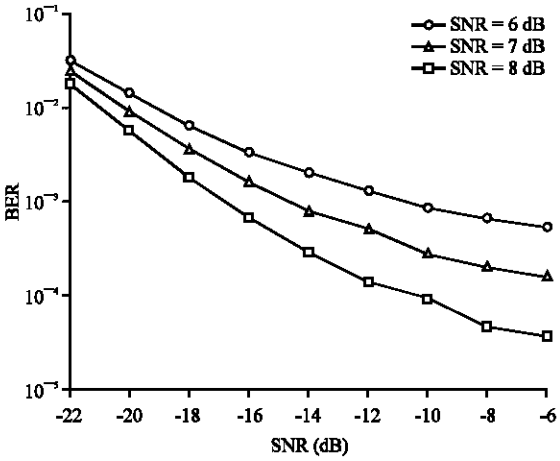

Fig. 9: USB receiver performance contrast curve

- When SNR is 6 dB, the BER of receiver without UWB interference is 3.8×10^{-4}, error rate can even reach 0.0307 after adding interference; the same, when SNR is 7 or 8 dB, the BER of receiver without UWB interference is 8.0×10^{-5} and 2.0×10^{-5}, error rate can even reach 0.0239 and 0.0173 after adding interference. This is due to SSA-UWB pulse design based on PSWF can fully cover the entire S-band so that the USB receiver will be interfered seriously
- As SNR increases, SIR threshold declines. Because SNR increasing can be seen as the exaltation of signal power, anti-jamming capability also will increase
- When SIR = -6 dB, SNR = 6, 7 and 8 dB, the BER of USB receiver is 5.32×10^{-4}, 1.54×10^{-4} and 3.6×10^{-5}. Visibly when the SIR is fixed, BER of the receiver increases with the SNR decreasing. This is because that USB transmitter signal power reduced with SNR decreasing, simultaneously interference power is constant, the performance of receiver is bound to reduce
- Observing any curve, the performance of USB receiver will deteriorate gradually with the interference signal power increasing gradually. When the SIR is less than the threshold of the normal working, the performance of USB receiver is very unstable and no longer available

The following research processes the UWB interference signal and analyzes the impact of the Unified S-band receiver in UWB signals of different firing intervals. Simulation analysis: Simulation parameters are same as above, SNR = 8 dB (it has the most powerful anti-interference ability), UWB interference firing interval is 5, 10 and 20 nsec. Figure 10 shows the different emission interval UWB waveform.

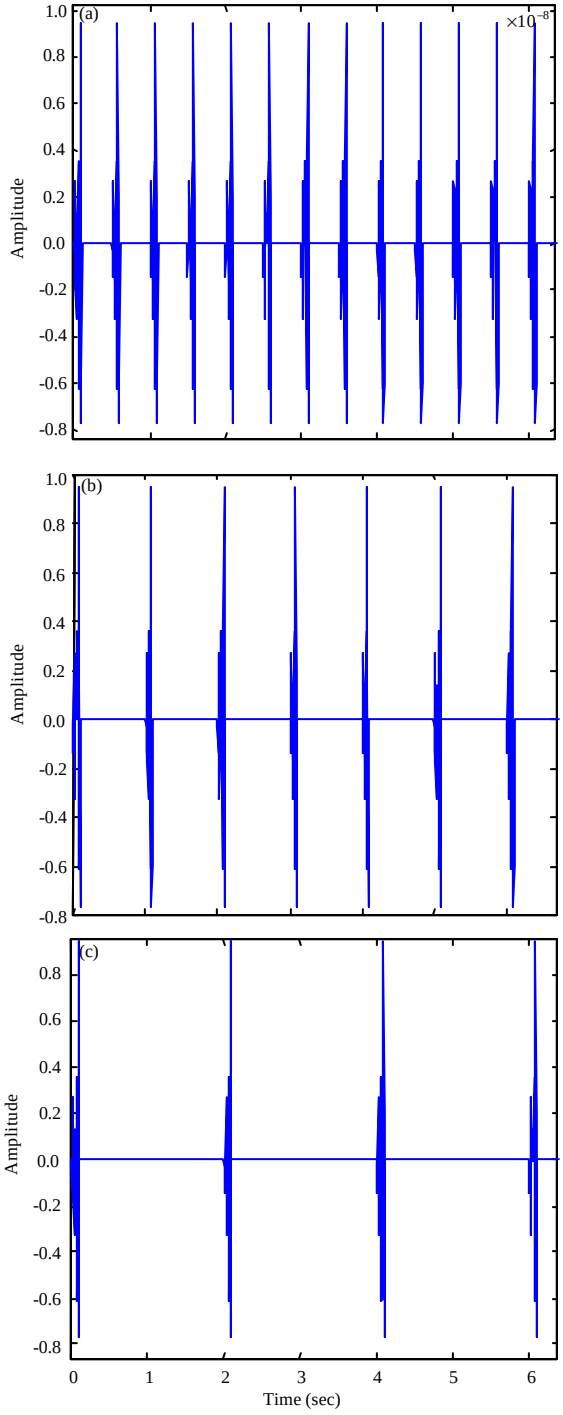

Fig. 10(a-c): UWB waveform of emission intervals, respectively (a) 5 nsec, (b) 10 nsec and (c) 20 nsec

When the SNR is 8 dB and the emission interval of UWB interference signal is 5, 10 and 20 nsec, the

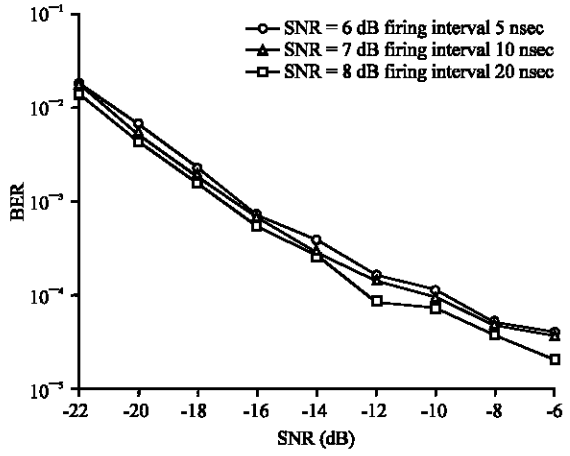

Fig. 11: USB receiver performance curve mixed in UWB interference

performance curve of the Unified S-band receiver is showed in Fig. 11. The SIR is the useful signal power divided by the interference signal power before the receiver band-pass filter. Analyze Fig. 11:

- When the firing interval of UWB interference signals increases to 20 nsec, the performance of the USB receiver is better than the situation of 5 and 10 nsec, but the degree of improvement is not obvious. Compare with the firing interval of 10 nsec, the SIR threshold value of normal work changes a little (2.5 dB) which is better than 10-5 nsec (increased by only 0.3 dB). Because the larger firing interval causes the lower power of interfering signals while the lower power of interfering signals results in weaker interference capability
- With the firing interval increasing, the improvement of the USB receiver performance is not obvious. But the interference of the USB receiver will be greatly enhanced when reducing the firing interval. The overall trend remains the same

CONCLUSION

This study first described the UWB pulse waveform based on Gaussian monocycle pulse. Then, it discussed the SSA pulse waveform optimization based on PSWF and used the power method to obtain the largest eigenvalues and eigenvectors in matrix operations. The UWB pulse waveforms which cover the entire S-band are used as interference signals. The transmitting and receiving model of Unified S-band receiver are designed and the performance of USB receiver is researched. This paper used BER to reflect the performance of the receiver, obtained the SNR and SIR threshold of USB receiver which can work properly and analyzed the influence of the firing interval of interfering signals.

REFERENCES

Di, J., S. Hong, Z. Qishan, Y. Li and K. Hong, 2010. Study on UWB cognitive radio using bridge function sequence matrix and PSWF pulse waveform. Proceedings of the 15th Conference on the Wireless Across the Taiwan Straits, September 2010, Kunming, China, pp: 6-9.

FCC, 2002. First Report and Order in the matter of revision of part 15 of the commission's rule regarding Ultra-wideband transmission system. FCC ET Docket, pp: 98-153.

Foerster, J., E. Green and S. Somayazulu, 2001. Ultra-wideband technology for short or medium-range wireless communications. Int. Technol. J. Q, 2: 1-11.

Honggang, Z. and R. Kohno, 2003. Soft spectrum adaptation in UWB impulse radio. Proceedings of the 14th IEEE International Symposium on Personal, Indoor and Mobile Radio Communications, Volume 1, September 7-10, 2003, Beijing, pp: 289-293.

Hua, S. and N.C. Beaulieu, 2011. Direct sequence and time-hopping sequence designs for narrowband interference mitigation in impulse radio UWB systems. IEEE Trans. Commun., 59: 1957-1965.

Lei, Z., Z. Chen, H. Wang, Z. Zhao and C. Liu, 2010. Multi-user capacity of M-PPM UWB system using PSWF pulses. Proceedings of the 3rd International Conference on Wireless, Mobile and Multimedia Networks, September 26-29, 2010, Beijing, China, pp: 86-89.

Li, Z., W. Zou, B. Li, Z. Zhou and X. Huang, 2011. Analysis on coexistence of ultra wideband with OFDM-based communication systems. IEEE Trans. Electromagn. Compat., 53: 823-830.

Liu, H. and J. Li, 2009. Terminal sliding mode control for spacecraft formation flying. IEEE Trans. Aerospace Electron. Syst., 45: 835-846.

Parr, B., B. Cho, K. Wallace and Z. Ding, 2003. A novel ultra-wideband pulse design algorithm. IEEE Commun. Lett., 7: 219-221.

Peng, Y., X. Wang, F. Ma and W. Sui. 2011. A low power S-band receiver using GaAs pHEMT technology. Proceedings of the 13th International Symposium on Integrated Circuits, December 12-14, 2011, Singapore, pp: 83-86.

Slepian, D., 1983. Some comments on Fourier analysis, uncertainty and modeling. SIAM Rev., 25: 379-393.

Wang, C., M. Ma, R. Ying and Y. Yang, 2010. Narrowband interference mitigation in DS-UWB systems. IEEE Signal Proc. Lett., 17: 429-432.

Wu, C., G. Jiang and H. Zhu, 2008. SSA realization for spectrum shaping and NBI suppression in cognitive UWB radios. Proceedings of the International Conference on Microwave and Millimeter Wave Technology, Volume 3, April 21-24, 2008, Nanjing, pp: 1454-1457.

Yin, Z., Y. Kuang, H. Sun, Z. Wu and W. Tang, 2012. A hybrid multiuser detection algorithm for outer space DS-UWB ad-hoc network with strong narrowband interference. KSII Trans. Internet Inf. Syst., 6: 1316-1332.